



## A 10 m vertical displacement on the Romanian Black Sea coast during modern history

Virgil Drăgușin<sup>1</sup>, Nicolaie Alexandru<sup>2</sup>, Mihai Caminschi<sup>1,3</sup>, Florina Chitea<sup>3,4</sup>, Vasile Ersek<sup>5</sup>, Alina Floroiu<sup>3</sup>, Liviu Giosan<sup>6,7</sup>, Georgiana Alexandra Grigore<sup>6,8,9</sup>, Diana Hanganu<sup>6</sup>, Maria Ilie<sup>10,11</sup>, Dumitru  
5 Ioane<sup>3</sup>, Marius Mocuța<sup>3</sup>, Adrian Iulian Pantia<sup>12</sup>, Iulian Popa<sup>3</sup>, Gabriela Sava<sup>10</sup>, Tiberiu Sava<sup>10</sup>, Răsvan Stochici<sup>3,4</sup>, and Constantin Ungureanu<sup>3</sup>

<sup>1</sup>Emil Racoviță Institute of Speleology, Romanian Academy, Bucharest, 010986, Romania

<sup>2</sup>Callatis Archaeology Museum, Mangalia, 905500, Romania

10 <sup>3</sup>Faculty of Geology and Geophysics, University of Bucharest, Bucharest, 010041, Romania

<sup>4</sup>Sabba S. Ștefănescu Institute of Geodynamics, Romanian Academy, Bucharest, 030167, Romania

<sup>5</sup>Department of Geography and Environmental Sciences, Northumbria University, Newcastle-upon-Tyne, NE1 8ST, United Kingdom

<sup>6</sup>Research Institute of the University of Bucharest, University of Bucharest, 050663, Romania

15 <sup>7</sup>Woods Hole Oceanographic Institution, Geology and Geophysics Department, Woods Hole, 02543, MA, USA

<sup>8</sup>Faculty of Biology, University of Bucharest, Bucharest, 050095, Romania

<sup>9</sup>National Institute of Research and Development for Biological Sciences, Bucharest, 060031, Romania

<sup>10</sup>Horia Hulubei National Institute for R&D in Physics and Nuclear Engineering, Măgurele, 077125, Romania

<sup>11</sup>Faculty of Physics, University of Bucharest, Măgurele, 077125, Romania

20 <sup>12</sup>Geological Institute of Romania, Bucharest, 012271, Romania

*Correspondence to:* Virgil Drăgușin ([virgil.dragusin@iser.ro](mailto:virgil.dragusin@iser.ro))

**Abstract.** Sea level reconstructions in the Black Sea basin and elsewhere rely on the identification of sea level markers and on the understanding of their post-genetic vertical movements. We present here evidence of a fast, bi-directional vertical displacement on the western Black Sea shore at Mangalia, Romania. We argue that an area situated near the shoreline was  
25 submerged 4 meters, subsequently filled with marine silts and sands, then uplifted by 10 m, where it currently stands. Radiocarbon dating of several types of materials from the infill, as well as archaeological evidence, indicate that this displacement occurred during the 18th-19th century. While performing radiocarbon dating, we found that near shore clam shells can show a <sup>14</sup>C reservoir age offset of ~900 years probably due to the hard water effect, adding more complications to the already problematic dating of Black Sea coastal sediments. Our findings offer strong evidence of short-term, local

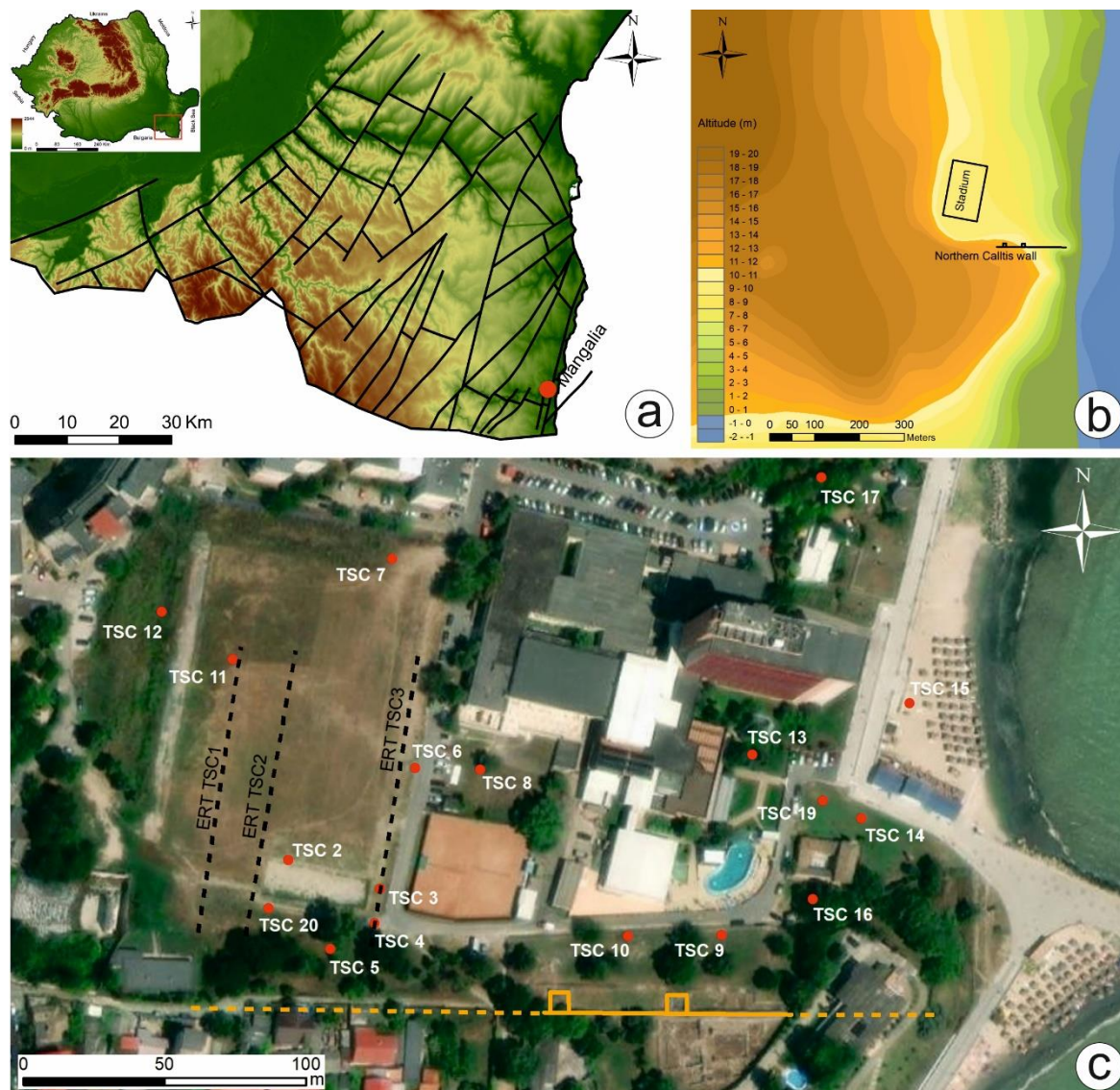


30 tectonic movements that should be considered when past sea levels are calculated, while at the same time serve a warning for  
urban and marine development planners.

## 1 Introduction

The region of Southern Dobrogea (Romania) is considered tectonically stable, as the geological history of this region has  
been interpreted not to show any vertical displacements or faulting since before the Miocene (Dinu et al., 2005).  
35 Nevertheless, offshore earthquakes were recorded during modern and historical times (Papadopoulos et al., 2011). The  
perception of long term tectonic stability influences the understanding of sea level indicators or of the dynamic of coastal  
settlements. For example, the definition of the Phanagorian regression in the Black Sea (1st millennium BCE) was based on  
the present day existence of submerged parts of the ancient city of Phanagoria several meters below sea level, on the Azov  
Sea coast. Likewise, at Mangalia (S Dobrogea), where the ancient city of Callatis existed (Fig. 1), the presence of ancient  
40 built structures 3 m below sea level led archaeologists to infer a low stand during the Antiquity (Alexandru et al., 2005).  
Giosan et al. (2006) showed that sea level has been relatively stable between -2 m and +1.5 m for the past 5000 years, and  
called for more detailed tectonic studies, as did Fouache et al. (2004) and Bruckner et al. (2010). Later, Fouache et al. (2012)  
thoroughly questioned the very existence of the Phanagorian regression based on the lack of neo-tectonic arguments.  
Recently, several studies revealed that the northern Black Sea coast experienced recurrent tectonic activity (Ovsyuchenko et  
45 al. 2017; 2018; 2019; 2020). Ovsyuchenko et al. (2018) offer a good example of tectonic effects on ancient settlements:  
Akra, on the shore of the Kerch Strait, was rapidly submerged when the wall of a strike-slip fault (with a normal fault  
component and a steep dip) sunk by a few meters.

Here we present a marine sediment deposit situated 10 m above sea level at Mangalia and argue that a fast, localized, high  
amplitude tectonic movement that took place in the 18th-19th centuries is responsible for its displacement.



50

**Fig. 1 – a.** Hypsometric map of S. Dobrogea with the main fault systems from Popa et al., (2019); **b.** Hypsometric map of Mangalia, with the stadium and the northern wall of Callitis; **c.** Location of cores and profiles (red dots), ERT profiles (dashed black lines), and the ancient wall (solid orange line - excavated, dashed orange line - buried). Base image: August 2022, Maxar/ESRI Map Viewer.

## 55 2 Results and discussion

### 2.1 Sediment infill

The sediment accumulation covers an area of ~20,000 m<sup>2</sup> and comprises four main stratigraphic units (Fig. 2a, Fig. S7-S16). The uppermost unit (Unit 1) is represented by a heterogeneous mixture of clay, limestone fragments and ceramics of



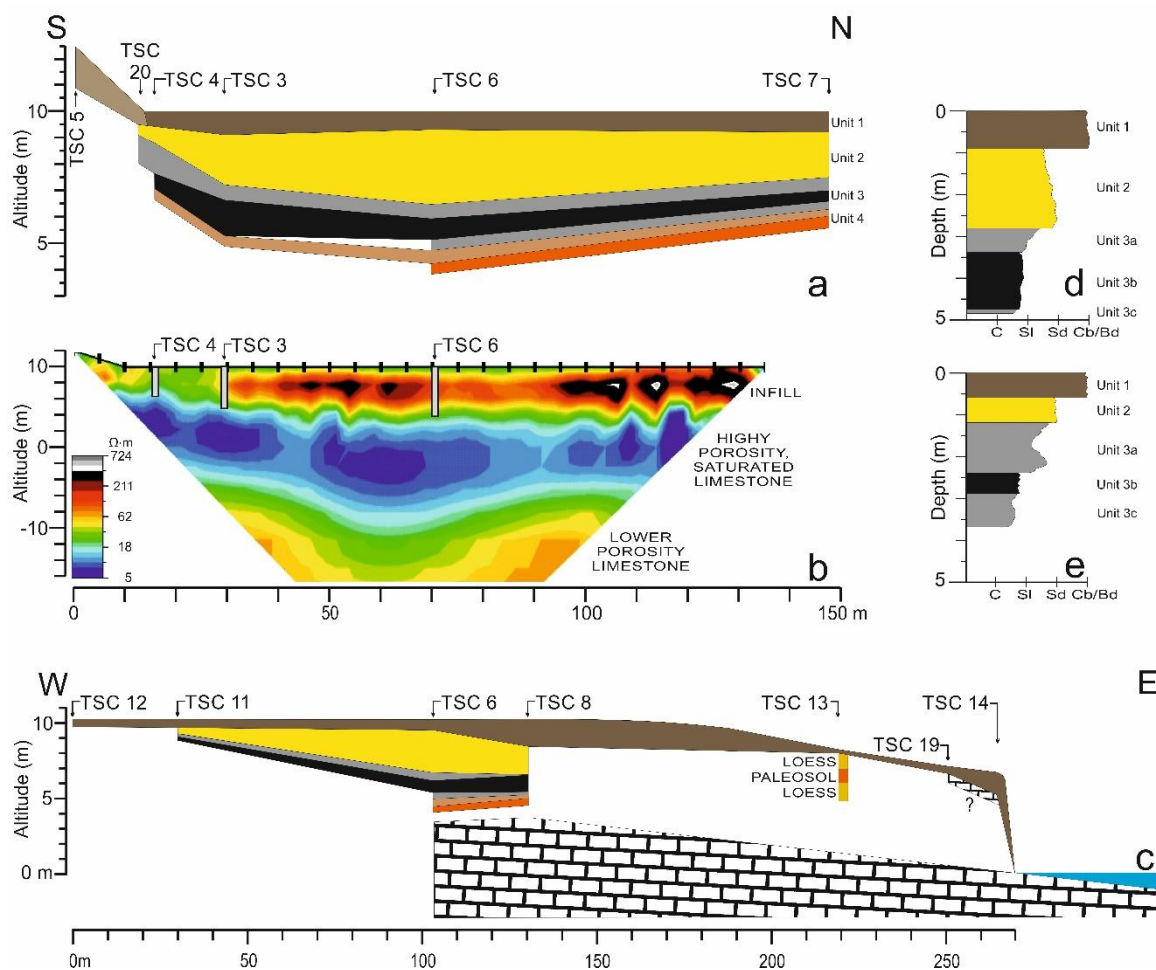
different origins, which is an infill emplaced during civil works in the 1950's. The thickness of this unit varies from 0.5 m at  
60 the western extremity of the studied area, to 1.8 m at the eastern edge (Fig. 2c). Unit 2 is comprised of sands with a thickness  
of up to 2.5 m, containing thin silt and clay layers (Table S2). It is the richest of all units in calcite (25%) and aragonite  
(36%), indicating a high shell component, quartz concentration being the lowest of all units (31%; Table S3). Unit 3  
(containing three sub-units) is a light grey clayey silt consisting mostly of quartz, with low concentrations of muscovite,  
calcite, and plagioclase.

65 In all profiles we found a dark grey to black clayey silt containing large quantities of fine charcoal (Unit 3b). At the southern  
edge of the sediment accumulation this unit contains large size elements such as fragments of roof tiles and other domestic  
use pottery, metal pieces, mussel shells (*Mytilus* sp.), and bone fragments. From among these we retrieved the bottom of a  
ceramic bowl coated on the interior with a green glaze (Fig. S13). It is specific for the Ottoman era (Guionova, 2022) that  
lasted from the early 15<sup>th</sup> to the late 19<sup>th</sup> century CE. In the southern part of the deposit, the charcoal rich layer is also the  
70 thickest, reaching 1.35 m at TSC3. In all profiles, it is underlain by light grey silt (Unit 3c) similar to Unit 3a, with a  
thickness of up to 80 cm.

Unit 4 is defined in TSC6 by the presence of a 0.5 m thick loess-like yellowish silt (Unit 4a) followed by 0.4 m of paleosol-  
like reddish clay (Unit 4b). In TSC7 and TSC8 the yellowish silt is replaced by a brownish clay that could be considered a  
buried soil, underlain by the reddish clay. Unit 4 consists of quartz, calcite, muscovite and chlorite, which is consistent with  
75 the mineralogical composition of nearby loess/paleosol sequences (Tugulan et al. 2016), thus implying that the marine  
sediment is underlain by thin loess/paleosol and patchy modern soil. None of the cores reached bedrock, although the coring  
at TSC4 stopped at 3.7 m on a hard surface.

At TSC13 we cored to a total depth of 3.4 m without reaching the bedrock and identified 2 main units: the 20<sup>th</sup> century  
anthropogenic infill, and a loess-paleosol sequence. Closer to the shore, we found the same anthropogenic infill in multiple  
80 cores with depths of up to 1.5 m overlaying a wide limestone surface with an area of at least 300 m<sup>2</sup>, which may not be part  
of the bedrock.

In all ERT transects, that reached up to 27 m below the surface, one can distinguish three units (Fig. 2b, Fig. S17). At the  
top, there is the marine sediment and anthropogenic infill, with a thickness growing eastward from ~2 m to ~7 m, as we also  
observed in our excavations and cores. A second, low resistivity unit (<10 Ωm), that we consider to represent highly porous,  
85 even vacuous, probably water saturated limestone with increased thickness towards the East. The third unit, with higher  
resistivity values, is probably a lower porosity limestone unit. The signal of the ground penetrating radar allowed for the  
depiction of the contact between Unit 1 and Unit 2 throughout the entire area (Fig. S18-S19).



90

**Fig. 2. a. S-N geological profile; b. ERT TSC 3 profile, with depiction of cores and profile location and depth; c. W-E geological profile d. TSC 3 lithological column; e. TSC 4 lithological column. C- clay, SI – silt, Sd – sand, Cb/Bd – cobbles/boulders.**

The sediment contains a large number of ostracods (*Amnicythere multituberculata*, *Loxoconcha* sp., *Leptocythere* sp., *Cyprideis littoralis*), foraminifera (*Ammonia beccarii*, *Elphidium* sp.), as well as mollusks (*Cerastoderma edule* and *Abra alba*), confirming their marine origin. None of the sediment units contain meaningful amounts of pollen or non-pollen palynomorphs, except for the archaeological layer (Unit 3b), where *Chenopodiaceae* and *Lactuceae* pollen is abundant. Coprophilous fungal taxa such as *Podospora*, *Sordaria*, and *Sporormiella*-type are well-represented, while *Chaetomium*, *Coniochaeta ligniaria*, and *Arnium*-type are less abundant (Table S4). This indicates an important dung input (van Geel et al., 2003; Cugny et al., 2010), probably from livestock in the village.

100



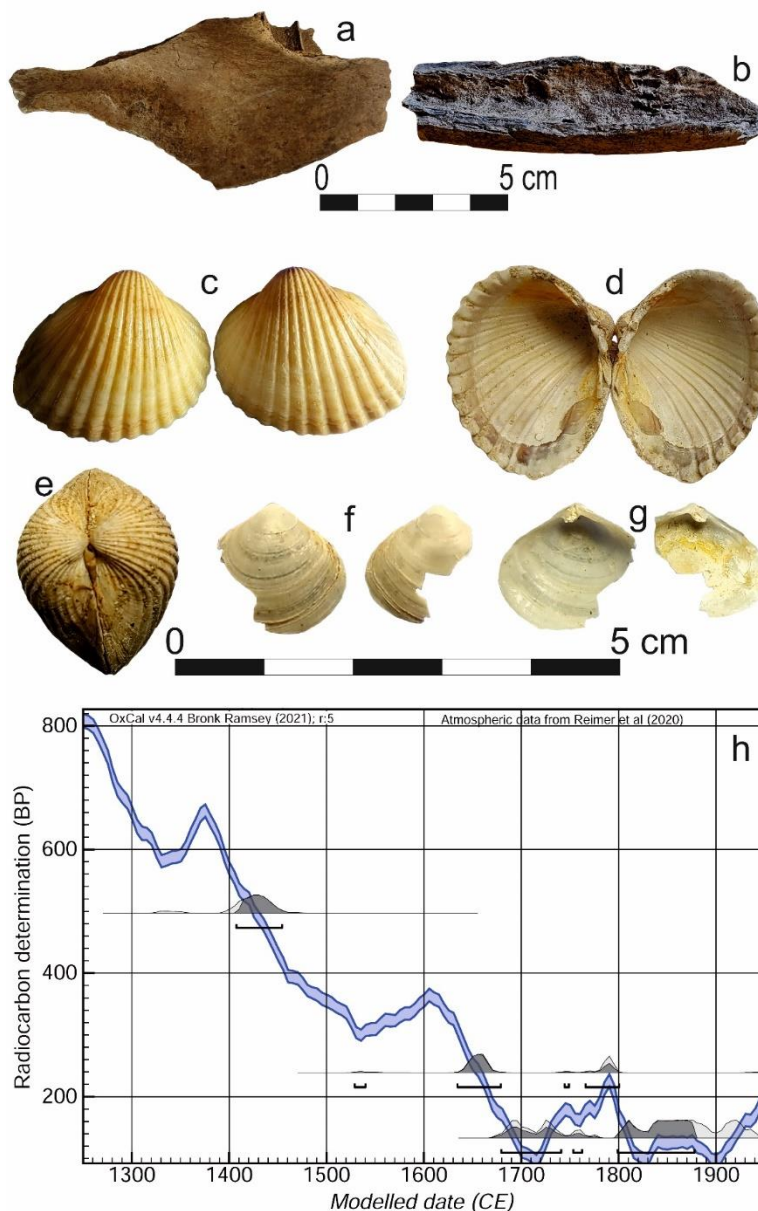


**Fig. 3 – Samples and dating results: a. TSC4-Os-01; b. TSC3 370cm; c. *C. edule*, lateral view; d. *C. edule*, internal view; e. *C. edule*, dorsal view; f. *A. alba*, lateral view; g. *A. alba*, internal view; h. Results of the calibration of TSC4-Os-01, TSC3 370cm, and TSC3 470cm on the Intcal20 curve.**

## 105 2.2 Chronology

Sample TSC3-470cm, a plant fragment from the contact of Unit 3c and Unit 4a returned the youngest  $^{14}\text{C}$  age,  $133 \pm 21$  yrBP (Table S5). Its C/N ratio (15.3) indicates a terrestrial origin, being closer to the domain of terrestrial C3 plants whose usual



values are  $>20$ , whereas marine and lacustrine algae have values  $<10$  (Meyers, 1994). A bone found in Unit 3b (TSC3-370cm, Fig. 4) returned a  $^{14}\text{C}$  age of  $239\pm 23$  yrBP, while another (TSC4-Os-01) returned a  $^{14}\text{C}$  age of  $497\pm 40$  yrBP. The  
110 C/N ratios of the two bone samples are specific for mammalian collagen (Deniro, 1985) and do not imply any diagenesis.  
The oldest  $^{14}\text{C}$  age,  $2971\pm 64$  yrBP, was obtained from a charcoal fragment (TSC4-Carb-01) in TSC4, 15 cm below the top of  
Unit 2 (Fig. S12). Shells of *C. edule* and *A. alba* found in anatomical connection at the same level in TSC4 yielded  $^{14}\text{C}$  ages  
of  $1066\pm 33$  yrBP and  $1018\pm 34$  yrBP, respectively. Two bulk sediment samples from Unit 3b have  $^{14}\text{C}$  ages of  $1114\pm 25$  yrBP  
and  $2435\pm 24$  yrBP, but such old age estimates are to be expected if the sediment incorporates reworked organic matter.  
115 The shell ages are more reliable than that of the charcoal as their presence in anatomical connection implies no reworking.  
Nevertheless, their stratigraphic position contradicts the age given by the plant material and requires further discussion.  
 $^{14}\text{C}$  ages of marine shells in the Black Sea are offset by reservoir ages that varied through the Holocene (Soulet et al., 2019)  
due to the fact that rivers contribute terrestrially-derived carbon of an older  $^{14}\text{C}$  age, which molluscs incorporate into their  
shells. Such terrestrial input can result in carbon stable isotope ( $\delta^{13}\text{C}$ ) values of shells as low as  $-10\%$  (VPDB), whereas  
120 marine carbon sourced from phytoplankton primary productivity, with direct atmosphere equilibration, results in shell  $\delta^{13}\text{C}$   
of  $\sim 0\%$ . A third source of carbon could originate in the activity of methanotrophs feeding in the sulphidic, methane rich  
springs that are widespread in Mangalia's coastal waters (Drăgușin et al., 2023), but would result in isotopic values lower  
than  $-40\%$  (Kessler et al., 2006; Soulet et al., 2018). Finally, a hard water effect could also be involved, due to the presence  
of underwater springs which drain the Sarmatian carbonate aquifer, whose water has  $^{14}\text{C}$  ages of about 12000 years  
125 (Davidescu et al., 1991). Five  $\delta^{13}\text{C}$  samples of the *C. edule* specimen and one sample of the *A. alba* specimen are between  
 $+0.03\%$  and  $-1.91\%$  (Table S6). This implies insignificant terrestrial or methanotrophic contributions, the mixing into the  
surface waters of spring-discharged hard water being, thus, the most probable explanation. Such an effect was also  
documented by Gomez et al. (2008) in other coastal settings. Based on the difference in  $^{14}\text{C}$  age between shells and the plant  
sample TSC3-470cm which predates them, the reservoir age could be as large as 900 years.

### 130 2.3 Evolution

As one might consider the possibility of these sediments being deposited by human action or by tsunami activity, we did not  
see any evidence of such origin. Our observations suggest that the original relief, covered by a patchy soil and loess cover,  
was situated close to the shore, when it rapidly subsided below the sea level, allowing the deposition of Unit 3c silts (Fig. 4).  
We consider, conservatively, that the terrain was close to sea level, in order for the submergence to have a minimum  
135 amplitude. During the early stage of the subsidence, debris from the village of Mangalia (charcoal, roof tiles, food remains as  
shells and bones, household ceramics, dung) started being discarded from the southern slope, at the base of which we found  
all large artefacts. The more buoyant, fine charcoal was spread by water and mixed into the silt matrix of Unit 3b, giving it  
the black coloration. After debris stopped being discarded, silt continued to deposit unabated, forming Unit 3a. Upon  
siltation and decreasing water depth, the sands of Unit 2 were deposited, in a beach-foreshore facies. The entire subsidence



140 amounted to at least 4 m, if we consider the original surface to have been above sea level. Finally, the entire area and the sediment infill were raised to the present day altitude of 9-10 m.

In order to estimate the timing of this two-phase displacement, the oldest age estimate of the submergence relies on the plant sample TSC3-470cm, which was probably growing in the soil of Unit 4. The bone sample TSC3-370cm, reworked from the village, predates the submergence. Calibration of  $^{14}\text{C}$  ages was performed in a sequence starting with TSC3-370cm, followed  
145 by TSC3-470cm, and the year 1878 as a boundary (Fig. 3). In 1878, Dobrogea became part of the Romanian Kingdom and began to be thoroughly studied by Romanian scientists who left no mention of this event, thus we presume it took place prior to 1878. Expression of calibrated ages using  $2\sigma$  probability (95.4%) returns two modelled date intervals for TSC3-370cm: 1630-1680 (72.8%) and 1760-1800 (20.6%). TSC3-470cm has two date intervals: 1670-1770 (29.5%) and 1790-1880 (65.9%). Thus, by taking a conservative approach, we argue that the submergence and emergence took place sometime  
150 between 1670 and 1878.

The submergence could have been the result of karst collapse, as the region around Mangalia is defined by the presence of large collapse dolines that are hundreds of meters in diameter (Lascu et al., 1995; Onac and Drăgușin, 2017; Drăgușin et al., 2021; 2023). Nevertheless, we do not consider the area of the stadium to be part of a collapse doline, as the ERT profiles do not indicate such morphology. This therefore points to a tectonic mechanism behind the submergence. Regarding the uplift,  
155 we do not envision other process but of tectonic origin. Thus, we consider both the subsidence and the uplift as swift results of tectonic activity taking place between 1670 and 1878.



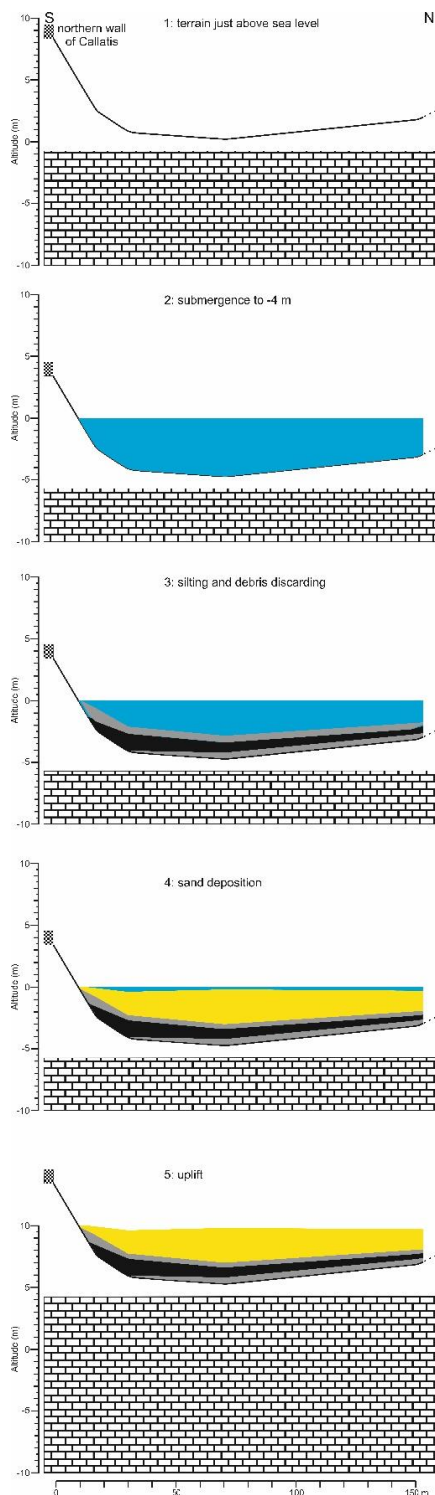


**Fig. 4 – Evolution model that considers the ancient city ruins to lay on the same tectonic block and to follow the same movements.**



### 3 Conclusions

160 Our results show that sea level markers can be affected to a large extent by tectonic movements. Taking into account recent  
studies on the northern shore of the Black Sea which identified similar tectonic movements (Ovsyuchenko et al., 2018; 2017;  
2020) and following the arguments of Giosan et al. (2006) and Fouache et al. (2012), we support the discarding of the  
Phanagorian Regression theory and other Black Sea level fluctuations that do not take into account tectonic movements. Our  
study also shows that neotectonic can be extremely recent, extremely abrupt, and could pose a high risk to coastal  
165 settlements.

#### Author contributions

Conceptualization: VD; Investigation: all authors; Visualization: VD; Writing – original draft preparation: all authors.

#### 170 Competing interests

The authors declare that they have no conflict of interest.

#### Acknowledgements

This research was supported by a grant of the Romanian Ministry of Education and Research, CNCS-UEFISCDI, project  
175 number PN-III-P4-ID-PCE-2020-2282. This work was supported under Research Programme Partnership in Priority Areas  
PNII MEN-UEFISCDI, contract PN 23210201 and PN 23210102. Experiments were carried out at 1 MV Tandetron™  
accelerator at Horia Hulubei National Institute for R&D Physics and Nuclear Engineering (IFIN-HH) and were supported by  
the Romanian Government Programme through the National Programme for Infrastructure of National Interest (IOSIN). We  
thank A. Iurkiewicz, C. Panaiotu and G. Anghel for helpful discussions, and the management of the Paradiso hotel for coring  
180 access.

### Appendix A.

#### Materials and Methods

185 The regional geology around Mangalia is represented by a Proterozoic basement and a carbonate sedimentary cover of  
Jurassic, Cretaceous, Eocene, and Miocene units (Feru and Capotă, 1991). A reviewed tectonic structure of the Southern  
Dobrogea Plateau was recently proposed by Popa et al. (2019) (Fig. 1a). Fault lines identified by Popa et al. (2019) are not  
represented at terrain surface, but at the top of the Valanginian (Lower Cretaceous) surface, which at Mangalia is at a depth  
of 150-250 m (Feru and Capotă, 1991).

190 The area around the town of Mangalia is dominated by the outcrops of sub-horizontally bedded Sarmatian (Miocene)  
limestones and marls, overlain by Pleistocene loess deposits. Recent work (Popa et al., 2024) revealed offshore fault lines



and a tilted tectonic block situated a few kilometres offshore. Two main aquifers are present in the area, an upper one hosted in the Sarmatian carbonates, and a lower one hosted in the Jurassic-Cretaceous carbonates. Faults and fractures allow mesothermal sulphidic water to rise and feed an aquifer hosted in the Sarmatian carbonates, the aquifer then draining through onshore and offshore springs. The interaction of the sulphidic waters, rich in H<sub>2</sub>S, with the carbonate host rock gave rise to hypogene karst features, the karst landscape extending below sea level (Onac and Drăguşin, 2017; Drăguşin et al., 2021; Drăguşin et al., 2023; Popa et al., 2024).

The marine sediments are found at an altitude of ~10 m a.s.l. and were exposed during an engineering project. Their stratigraphy is described from several open profiles (TSC2, TSC3, TSC4, TSC11, TSC12, and TSC20), while at the other points we used a small diameter hand auger to investigate the sediments (Fig. 1c; Table S1). Electrical resistivity tomography (ERT) and ground penetrating radar were used to study the extent of the sediment accumulation, as well as to infer the depth to bedrock. We analysed the grain size, mineralogy, and electrical conductivity of the sediment, as well as fauna, pollen, and non-pollen palynomorphs.

The **grain size analysis** of profiles TSC 3 and TSC 4 was performed according to the ISO 17892-4:2016 standard – „Laboratory testing of soil – Determination of particle size distribution”. Initial wet sieving was performed on the 0.063mm sieve to separate the coarse fraction from the fine fraction. The fine fraction was analysed using the hydrometer method and the coarse particles by dry sieving.

**Mineralogy** was analysed by means of X-ray powder diffraction, using a Bruker D8 Advance diffractometer with a vertical goniometer,  $\theta$ -2 $\theta$  configuration (Bragg-Bretano geometry), and Cu anode. The optical path of the 1.5406 Å X-ray beam was defined by 0.6 mm divergent and receiving slits, a 0.2 mm detector slit, and a Ni filter located between the receiving and detector slits. The measurements were performed at 40 kV and 40 mA over a 2 $\theta$  interval of 4-90° with a 0.04° increment and a 1s/increment acquisition time. The investigated samples were bathed in acetone in order to remove some of the organic matter and prevent unnecessarily high background signals (acids were not used so as not to dissolve the carbonaceous material expected in the samples), and manually ground to a fine, talc-like powder (<0.062 mm) using a mortar. The diffractograms were interpreted using the Diffrac<sup>+</sup> Basic (Eva 13) dedicated software.

**<sup>14</sup>C dating** was performed on different materials (bulk sediment, charcoal, bone, plant remains, and bivalve shells) extracted from profiles TSC3 and TSC4 (Table S2), at the ROAMS laboratory in Măgurele, Romania. For charcoal, plant remains, and sediment, we used the standard acid-base-acid (ABA) protocol described by Sava et al. (2018). The standard pre-treatment method for shells involved surface cleaning by rinsing with ultrapure water and then washing with a gentle (HCl) acid solution using ultrasonication to remove the outer carbonate layer, which may have recrystallized and at the end rinsed with ultrapure water. For the graphitization stage we used an AGE III automated system (Wacker et al. 2010a) which worked in conjunction with an elemental analyser (Vario MicroCube, Elementar, Germany) for combustion of the organics and with a carbonate digestion system, Carbonate Handling System (CHS, IonPlus AG, Switzerland, Wacker et al. 2013) for the inorganics samples.



225 The AMS measurements were performed on a 1 MV Tandemtron HVEE AMS system. All the samples were normalized against NIST SRM 4990C – Oxalic Acid II (NIST 1983) to the modern radiocarbon level. To estimate the blank level an old charcoal of unknown source was used for the organics, or IAEA-C1 marble for inorganic samples. By measuring the  $^{13}\text{C}/^{12}\text{C}$  ratio, all the  $^{14}\text{C}/^{12}\text{C}$  isotopic ratios were  $\delta^{13}\text{C}$  corrected for natural and induced fractionation. The data analysis was performed using the BATS software tool (Wacker et al. 2010b) in accordance with Stuiver and Polach (1977).

230 For the chronology of the marine sediment accumulation, calibration was performed only on the plant, bone, and charcoal materials, using the OxCal v4.4.4 program (Bronk-Ramsey, 2009) and the IntCal20 calibration curve (Reimer et al., 2020), as well as the post-bomb atmospheric NH1 curve (Hua et al., 2022), which resulted in mostly similar calibrations.

**Stable isotope measurements** of carbon were performed on two bivalve shells in order to support their radiocarbon dating. The analysis was carried out at the Northumbria University stable isotope laboratory, which uses an analysis method adapted from Spötl and Venneman (2003). Samples were loaded into 12 mL borosilicate vials capped with butyl rubber septa (LabcoTM), and flushed with helium for 480 seconds at 1.8 bar on a bespoke flushing box supplied by Sercon Ltd. Carbon, in a Thermo GasBench II sample preparation device. Measurements were performed on a Thermo Delta V Advantage IRMS. Individual measurement sequences consisted of 80 measurements, including standards, and all samples were reacted with 102 wt% orthophosphoric acid at a temperature of 70°C, with a reaction time of 104 minutes prior to measurement to ensure 235 equilibration. For data evaluation, standards were measured at the beginning, end, and approximately every 10 samples in each sequence. An in-house laboratory calcite standard (Plessen) was used for linearity and drift correction ( $\delta^{13}\text{C} = 2.40\text{‰}$ ,  $\delta^{18}\text{O} = -1.31\text{‰}$ ,  $n = 10$  per sequence), alongside international standards NBS18 and IAEA603 for stretching correction (each  $n \geq 3$  per sequence). Nominal values from Kim et al. (2015) were used for NBS18 ( $\delta^{13}\text{C} = -5.01\text{‰}$ ,  $\delta^{18}\text{O} = -23.01\text{‰}$ ), while values stated by the IAEA were used for IAEA603 ([www.iaea.org](http://www.iaea.org);  $\delta^{13}\text{C} = 2.46\text{‰}$ ,  $\delta^{18}\text{O} = -2.37\text{‰}$ ). One sample of an 245 in-house calcite standard (Pol2,  $\delta^{13}\text{C} = -7.14\text{‰}$ ,  $\delta^{18}\text{O} = -9.22\text{‰}$ ) was added to each sequence and used to evaluate long-term performance. Based on this secondary standard, for the measurement period relevant to the samples reported here, reproducibility is better than 0.1‰ for both  $\delta^{13}\text{C}$  and  $\delta^{18}\text{O}$ . All stable isotope data are reported on the VPDB scale.

**Ground penetrating radar** used antennas with central frequencies of 200MHz and 600MHz. **Electrical resistivity tomography** measurements were performed on three parallel transects oriented S-N. Measurements were made in the same 250 day, at a short time-interval difference, permitting an adequate evaluation of the determined parameter variation even for top-part areas which are more prone to reflect external influences if climatic conditions changes.

## References

- Alexandru, N., Constantin, R., and Ionescu M.: Aspecte topografice ale cetății Callatis, Pontica, 37–38, 419–38, 2005
- 255 Bronk Ramsey, C.: Bayesian analysis of radiocarbon dates, *Radiocarbon*, 51(1), 337-360, doi:10.1017/S0033822200033865, 2009.



- Brückner, H., Kelterbaum, D., Marunchak, O., Porotov, A., and Vött, A.: The Holocene sea level story since 7500 BP–  
Lessons from the Eastern Mediterranean, the Black and the Azov Seas, *Quat. Int.*, 225(2), 160–179,  
doi:10.1016/j.quaint.2008.11.016, 2010
- 260 Cugny, C., Mazier, F., and Galop, D.: Modern and fossil non-pollen palynomorphs from the Basque mountains (western  
Pyrenees, France): the use of coprophilous fungi to reconstruct pastoral activity, *Veg. Hist. Archaeobot.*, 19, 391–408,  
doi:10.1007/s00334-010-0242-6, 2010.
- Davidescu, F. D., Țenu, A., and Slăvescu, A.: Environmental isotopes in karst hydrology. A lay-out of problems with  
exemplifications in Romania, *Theoretical and Applied Karstology*, 4, 77–86, 1991.
- 265 Deniro, M. J.: Postmortem preservation and alteration of in vivo bone collagen isotope ratios in relation to palaeodietary  
reconstruction, *Nature*, 317, 806–809, doi:10.1038/317806a0, 1985.
- Dinu, C., Wong, H. K., Tambrea, D., and Matenco, L.: Stratigraphic and structural characteristics of the Romanian Black  
Sea shelf, *Tectonophysics*, 410 (1–4), 417–35, doi:10.1016/j.tecto.2005.04.012, 2005.
- Drăgușin, V., Tîrlă, L., Covaliov, S., Cruceru, N., Mirea, I. C., and Șandric, I.: The unique topography from Obantul Mare  
270 (Mangalia, SE Romania): remnant of a maze cave, *Géomorphol. Relief Process. Environ.*, 27 (3), 221–229,  
doi:10.4000/geomorphologie.15794, 2021.
- Drăgușin, V., Vlaicu, M., Balan, S. V., Baci, M., Pop, M. M., and Sambor, A. O.: Characteristics of submerged and  
partially submerged caves (habitat type 8330) in Romania, *Environ. Monit. Assess.*, 195 (12), 1520,  
doi:10.1007/s10661-023-12137-1, 2023,
- 275 Feru, M. U., and Capotă, A.: Les eaux thermominerales karstiques de la zone de Mangalia (Roumanie), *Theoretical and  
Applied Karstology*, v. 4, p. 143–157, 1991.
- Fouache, E., Porotov, A., Muller, C., and Gorlov, Y.: The role of neo-tectonics in the variaton of the relative mean sea level  
throughout the last 6000 years on the Taman Peninsula (Black Sea, Azov Sea, Russia), in: *Proceedings of the  
conference "Rapid transgressions into semi-enclosed basins"*, edited by: Uścińowicz, S., Balabanis, P., Kramarska, R.,  
280 Zachowicz J., Polish Geological Institute Special Papers, 11, 47–58, 2004.
- Fouache, E., Kelterbaum, D., Brückner, H., Lericolais, G., Porotov, A., and Dikarev V.: The Late Holocene evolution of the  
Black Sea - a critical view on the so-called Phanagorian Regression, *Quat. Int.*, 266, 162–74,  
doi:10.1016/j.quaint.2011.04.008, 2012.
- Giosan, L., Donnelly, J. P., Constantinescu, S., Filip, F., Ovejano, I., Vespremeanu-Stroe, A., Vespremeanu, E., and Duller,  
285 G. A. T.: Young Danube Delta documents stable Black Sea level since the Middle Holocene: morphodynamic,  
paleogeographic, and archaeological implications, *Geology*, 34 (9), 757–760, doi:10.1130/G22587.1, 2006.
- Guionova, G.: Daily material life in Sofia through locally produced ceramics, 15th–19th centuries, *Archaeol.Bulg.*, 26 (2),  
117–137, 2022.
- Hua, Q., Turnbull, J. C., Santos, G. M., Rakowski, A. Z., Ancapichún, S., De Pol-Holz, R., Hammer, S., Lehman, S. J.,  
290 Levin, I., Miller, J. B., Palmer, J. G., and Turney, C. S. M.: Atmospheric Radiocarbon for the Period 1950–2019,





- Radiocarbon, 64 (4), 723–745, doi:10.1017/RDC.2021.95, 2022.
- IAEA: RS IAEA-C1 to IAEA-C9 Rev.01., Reference sheet for quality control materials, 2014.
- Kessler, J. D., Reeburgh, W. S., Southon, J., Seifert, R., Michaelis, W., and Tyler, S. C.: Basin-wide estimates of the input of methane from seeps and clathrates to the Black Sea, *Earth Planet. Sci. Lett.*, 243 (3–4), 366–375, doi:10.1016/j.epsl.2006.01.006, 2006.
- 295 Kim, S.-T., Coplen, T. B., and Horita, J.: Normalization of stable isotope data for carbonate minerals: Implementation of IUPAC guidelines, *Geoch. Cosmochim. Ac.*, 158, 276–289, doi:10.1016/j.gca.2015.02.011, 2015.
- Lascu, C., Popa, R., and Sarbu, S.: Le karst de Movile (Dobrogea de Sud) (II), *Rev. Roum.de Geogr.*, 39, 31–40, 1995.
- Meyers, P. A.: Preservation of elemental and isotopic source identification of sedimentary organic matter, *Chem. Geol.*, 114  
300 (3–4), 289–302, doi:10.1016/0009-2541(94)90059-0, 1994.
- NIST: SRM 4990C International Standard Reference Material for Contemporary Carbon-14, 1983.
- Onac, B. P., and Drăgușin, V.: Hypogene Caves of Romania, in: *Hypogene Karst Regions and Caves of the World, Cave and Karst Systems of the World*, edited by: Klimchouk, A., Palmer, A. N., De Waele, J., Auler, A. S., and Audra, P., Springer, 257–265, doi:10.1007/978-3-319-53348-3\_16, 2017.
- 305 Ovsyuchenko, A. N., Korzhenkov, A. M., Larkov, A. S., Marahanov, A. V., and Rogozhin, E. A.: New findings on the sources of strong earthquakes in Kerch Peninsula based on paleoseismological data, *Dokl. Earth Sci.*, 472 (1), 53–56, doi:10.1134/S1028334X17010081, 2017.
- Ovsyuchenko, A. N., Korzhenkov, A. M., Larkov, A. S., Marahanov A. V., and Rogozhin, E. A.: Estimation of seismic hazards of low-active areas: case study of Kerch–Taman region, *Seism. Instrum.*, 54 (5), 565–572,  
310 doi:10.3103/s0747923918050109, 2018.
- Ovsyuchenko, A. N., Novichikhin, A. M., Bykhalova, O. N., Rogozhin, E. A., Korzhenkov, A. M., Larkov, A. S., Butanaev, Y. V., and Lukashova, R. N.: Interdisciplinary dating of Utrish seismic dislocations: localization of the source of a strong historical earthquake in the Western Caucasus, *Seism. Instrum.*, 56 (2), 174–193,  
doi:10.3103/S0747923920020097, 2020.
- 315 Ovsyuchenko, A. N., Vakarchuk, R. N., Korzhenkov, A. M., Larkov, A. S., Sysolin, A. I., Rogozhin, E. A., and Marakhanov, A. V.: Active faults in the Kerch Peninsula: new results, *Dokl. Earth Sci.*, 488 (2), 1152–1156, doi:10.1134/S1028334X19100076, 2019.
- Papadopoulos, G. A., Diakogianni, G., Fokaefs, A., and Rangelov, B.: Tsunami hazard in the Black Sea and the Azov Sea : a new tsunami catalogue, *Nat. Hazard. Earth Sys. Sci.*, 11, 945–963, doi:10.5194/nhess-11-945-2011, 2011.
- 320 Popa, I., Mocuța, M., and Iurkiewicz, A.: A new regional conceptual model on the hydrogeology of Southern Dobrogea based on seismic surveys and hydro-geological data revisiting, in: *Proceedings of 4th Conference of the IAH CEG*, edited by: Stevanovic, Z., Zivanovic, V., and Milanovic P., International Association of Hydrogeologists (IAH) National Chapter (NC) of Serbia, 47–49, 2019.
- Popa, A., Stanciu, I. M., Drăgușin, V., Teacă, A., Balan, S., V., Popa, M. E., Ion, G., and Ispas, B. A.: Geophysical and



- 325 geochemical investigations of underwater sulphurous seeps from Western Black Sea (Mangalia area, Romania), in support of habitat conservation. *Front. Mar. Sci.*, 11:1414673, doi:10.3389/fmars.2024.1414673, 2024.
- Reimer, P. J., Austin, W. E. N., Bard, E., Bayliss, A., Blackwell, P. G., Bronk Ramsey, C., Butzin, M., Cheng, H., Edwards, R. L., Friedrich, M., Grootes, P. M., Guilderson, T. P., Hajdas, I., Heaton, T. J., Hogg, A. G., Hughen, K. A., Kromer, B., Manning, S. W., Muscheler, R., Palmer, J. G., Pearson, C., Van Der Plicht, J., Reimer, R. W., Richards, D. A.,  
330 Scott, E. M., Southon, J. R., Turney, C. S. M., Wacker, L., Adolphi, F., Büntgen, U., Capano, M., Fahrni, S. M., Fogtmann-Schulz, A., Friedrich, R., Köhler, P., Kudsk, S., Miyake, F., Olsen, J., Reinig, F., Sakamoto, M., Sookdeo, A., and Talamo, S.: The IntCal20 Northern Hemisphere radiocarbon age calibration curve (0-55 cal kBP), *Radiocarbon*, 62(4), 725–757, doi:10.1017/RDC.2020.41, 2020.
- Sava, T., Simion, C., Gâza, O., Stanciu, I., Păceșilă, D., Wacker, L., Ștefan, B., Moșu, V., Ghiță, D., and Vasiliu, A.: Status  
335 report on the sample preparation laboratory for radiocarbon dating at the new Bucharest RoAMS center, *Radiocarbon*, 61, 649–658, doi:10.1017/RDC.2018.123, 2018.
- Soulet, G., Giosan, L., Flaux, C., and Galy, V.: Using stable carbon isotopes to quantify radiocarbon reservoir age offsets in the coastal Black Sea, *Radiocarbon*, 61 (1), 309–318, doi:10.1017/RDC.2018.61, 2019.
- Spötl, C., and Vennemann, T.W.: Continuous-flow isotope ratio mass spectrometric analysis of carbonate minerals, *Rapid  
340 Commun. Mass Spectrom.*, 17, 1004–1006, doi:10.1002/rcm.10102003, 2003.
- Stuiver, M., and Polach, H.: Discussion: reporting of  $^{14}\text{C}$  data, *Radiocarbon*, 19 (3), 355–363, 1977.
- Tugulan, L. C., Dului, O. G., Bojar, A. V., Dumitras, D., Zinicovskaia, I., Culicov, O. A., and Frontasyeva, M. V.: On the geochemistry of the Late Quaternary loess deposits of Dobrogea (Romania), *Quat. Int.*, 399, 100–110, doi:10.1016/j.quaint.2015.06.062, 2016.
- 345 van Geel, B., Buurman, J., Brinkkemper, O., Schelvis, J., Aptroot, A., van Reenen, G., and Hakbijl, T.: Environmental reconstruction of a Roman Period settlement site in Uitgeest (The Netherlands), with special reference to coprophilous fungi, *J. Archaeol. Sci.*, 30 (7), 873–883, doi:10.1016/S0305-4403(02)00265-0, 2003.
- Wacker, L., Němec, M., and Bourquin, J.: A revolutionary graphitization system: fully automated, compact and simple, *Nucl. Instr. Meth. B.*, 268, 931–934, 2010a.
- 350 Wacker, L., Christl, M., and Synal, H.-A.: BATS: A new tool for AMS data reduction, *Nucl. Instr. Meth. B.*, 268, 976–979, 2010b.
- Wacker, L., Fülöp, R.H., Hajdas, I., Molnar, M., and Rethemeyer, J.: A novel approach to process carbonate samples for radiocarbon measurements with helium carrier gas, *Nucl. Instr. Meth. B.*, 294, 214–217, 2013.